

TRANSFORMER MODELING TAKING INTO ACCOUNT HYSTERESIS BEHAVIOR

Wolfgang Baumgartinger^(a), Manfred Kaltenbacher^(b), Mario Jungwirth^(c)

^(a,c)Department of Automation Engineering, University of Applied Science Wels, Austria

^(b)Institute of Mechanics and Mechatronics, Vienna University of Technology, Austria

^(a) wolfgang.baumgartinger@fh-wels.at, ^(b) manfred.kaltenbacher@tu-wien.ac.at, ^(c) mario.jungwirth@fh-wels.at

ABSTRACT

An efficient and precise finite network model to simulate the dynamic behaviour of transformer core laminations is presented. The model considers both hysteresis and eddy current losses and is based on an electric and magnetic circuit connected by a gyrator. This approach allows to easily include the classical Preisach operator to take into account hysteresis and saturation behaviour. The eddy current losses are modelled with an additional inductance in the magnetic circuit. Simulation results are in good agreement with measurements of a single phase and three phase transformer as used in power-supply systems.

Keywords: Preisach Model, Hysteresis, Transformer

1. INTRODUCTION

The design of energy-efficient power transformers and electric power systems requires a mathematical model of sufficient complexity (Jungwirth, Baumgartinger, and Kaltenbacher 2010). In case of fault detection the phenomenon of inrush current in transformers has been known for many years, and discussed in many studies (Akçay and Ece 2003; Casoria, Sybille, and Brunelle 2003; Chen, Lin, and Cheng 2005; Theocharis, Miliaris-Argitis, and Zacharias 2008). The well-known linear transformer model does not take the effects of saturation, hysteresis and eddy currents into consideration. However, these nonlinearities significantly influence the behavior of a transformer during switching-on and restart as well as other types of transients (Akçay and Ece 2003).

The current research work was motivated from the objective of precisely estimating the dynamic behavior of transformers, and therefore hysteresis, saturation and eddy currents are taken into account. The parameters for our model are determined from measurements performed on an Epstein frame or/and directly on the transformer cores itself, and the SimPowerSystems-Toolbox in MATLAB/Simulink is used as simulation environment. The developed model is applied to a single phase and a three phase transformer.

2. TRANSFORMER

2.1. Ideal Transformer Model

A transformer is an electric device that transfers energy from one circuit to another. The two circuits are coupled

by a magnetic field, which is mainly concentrated within the iron core. The simplest model considers this iron core as ideal. This means that the transformer has no losses, and so the energy transfer from the primary side to the secondary side is perfect.

A transformer consists of the primary side with N_1 windings and the secondary side with N_2 windings. If a time-varying voltage u_1 is applied to the primary side, a current will flow and produces a magnetomotive force (MMF). The MMF drives the varying magnetic flux ϕ_1 through the iron core and induces a back electromotive force (EMF) in opposition to u_1 . In accordance with Faraday's law, the voltage induced across the primary winding is proportional to the rate of change of flux

$$u_1 = N_1 \frac{d\phi_1}{dt}. \quad (1)$$

Therefore, the voltage induced across the secondary winding is

$$u_2 = N_2 \frac{d\phi_2}{dt}. \quad (2)$$

If and only if a perfect flux coupling is available, the flux on the primary side will be equal to the flux in the secondary side. So we can equate ϕ_1 and ϕ_2 and obtain the following fundamental relation

$$\frac{u_1}{u_2} = \frac{N_1}{N_2} = \frac{i_2}{i_1} = \ddot{u}. \quad (3)$$

2.2. Non-Ideal Transformer model

For a realistic transformer model we have to consider the magnetic resistance of the iron core and its losses (Hagmann 2001). The losses can be represented by an iron loss resistance R_{Fe} in parallel with the main impedance L_H , see Fig. 2. The resistance characterizes the iron core losses and the impedance describes the magnetizing current I_μ which maintains the mutual flux in the core. The sum of the magnetizing current and the current through the resistance R_{Fe} describes the unloaded transformer with the no-load current I_{10} .

Furthermore, the windings of the transformer are magnetically non-ideal coupled with each other, which results in flux leakage as shown in Fig. 1.

This can be modeled as reactances of each leakage inductance $L_{\sigma 1}$ and $L_{\sigma 2}$. Taking into account the power

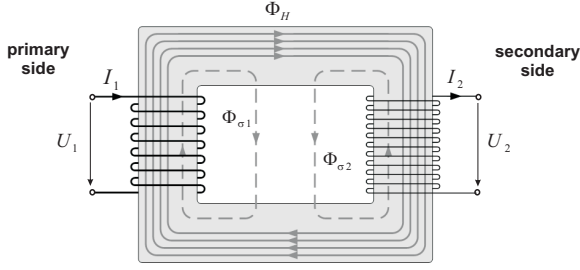


Figure 1: Flux Leakage in a Transformer.

loss in the windings R_1 and R_2 , which are represented as in-series resistances to the leakage inductances, the equivalent circuit diagram of a real transformer is displayed in fig 2.

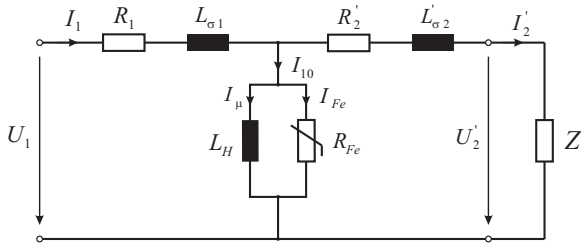


Figure 2: Equivalent Circuit Model for the Non-Ideal Transformer.

All elements on the secondary side can be converted to the primary side using (3). Therefore, R'_2 , $L'_{\sigma 2}$, I'_2 , U'_2 and Z' compute as

$$R'_2 = \ddot{u}^2 R_2 \quad (4a)$$

$$L'_{\sigma 2} = \ddot{u}^2 L_{\sigma 2} \quad (4b)$$

$$I'_2 = \frac{1}{\ddot{u}^2} I_2 \quad (4c)$$

$$U'_2 = \ddot{u}^2 U_2 \quad (4d)$$

$$Z' = \ddot{u}^2 Z. \quad (4e)$$

2.3. Transformer Equations for Inrush Currents

The general solution of the differential equation for the primary side of the single-phase transformer is

$$u_1 = R_1 i_1 + L_{\sigma 1} \frac{di_1}{dt} + \frac{d\psi}{dt}, \quad (5)$$

where ψ denotes the total linked flux, which computes as

$$\psi = N\phi = L_H i_\mu. \quad (6)$$

Inserting (6) into (5) results in

$$u_1 = R_1 i_1 + L_{\sigma 1} \frac{di_1}{dt} + i_\mu \frac{dL_H}{dt} + L_H \frac{di_\mu}{dt}. \quad (7)$$

Therefore, neglecting the leakage flux ($L_{\sigma 1} \frac{di_1}{dt}$), and the iron loss resistance (R_{Fe}) simplifies (7) to

$$u_1 = R_1 i_1 + L_H \frac{di_\mu}{dt}. \quad (8)$$

This relation will be used in the simulation to determine the inrush currents.

3. PREISACH MODEL

Various methods have been proposed for modeling hysteresis (Mayergoyz 2003; Visintin 1994; Krasnoselskii and Pokrovskii 1989). However, due to its universality, the most practical approach to model hysteresis behavior is provided by the Preisach operator. Mayergoyz was the first who described a method to identify the density function for the Preisach operator in the proof of his characterization theorem (for details, see (Mayergoyz 2003)). The important weight matrix, which is computed by the density function, is based on data supplied from manufacturers and/or obtained from defined measurements, e.g., by an Epstein frame.

3.1. Basic definitions

In the following section, we will describe the Preisach operator, and discuss its properties. Let's consider the non-ideal relay operator $\gamma_{\alpha\beta}$ which is characterized by its threshold values $\alpha > \beta$. Its output $\gamma_{\alpha\beta}$ can take the values 0 or 1 where α is the 'ON switch' and β the 'OFF switch' of the operator. The dynamics of the relay are illustrated by Fig. 3.

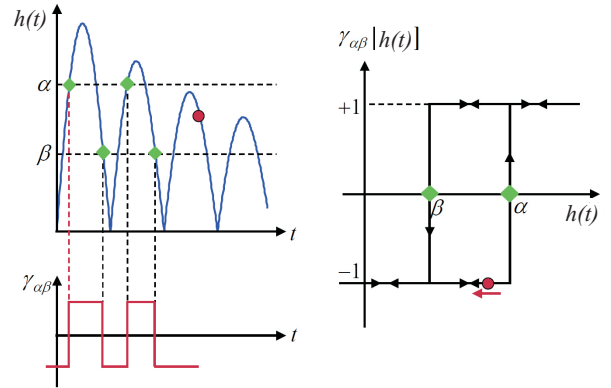


Figure 3: Simplest Hysteretic Operator.

The values of the output of $\gamma_{\alpha\beta}$ at a moment t_k are defined by the following explicit formula:

$$\gamma_{\alpha\beta}[h(t_k)] = \begin{cases} +1 & h(t_k) > \alpha, \\ \gamma_{\alpha\beta}[h(t_k - 1)] & \beta > h(t_k) > \alpha, \\ -1 & h(t_k) < \beta. \end{cases} \quad (9)$$

where $h(t_k)$ is the input value at time t_k .

The main assumption made in the Preisach model (Mayergoyz 2003) is that the system can be thought of as the parallel summation of a continuum of such weighted

non ideal relays $\gamma_{\alpha\beta}$, where the weighting of each relay is $\wp(\alpha, \beta)$. Such a summation can be uniquely represented as a collection of non-ideal relays as points on the two-dimensional half-plane $S = \{(\alpha, \beta) \in \mathbb{R}^2 | \alpha \geq \beta\}$. This is also known as the Preisach plane and is displayed in Fig. 4. Here the area S^+ is the set of the threshold values (α, β) for which the corresponding relays $\gamma_{\alpha\beta}$ are switched on at a given moment t . The output of the Preisach model $\mathcal{H}(t)$ then computes as

$$\mathcal{H}(t) = B(t) = B_s \iint_S \wp(\alpha, \beta) \gamma_{\alpha\beta} [h(t_k)] d\alpha d\beta, \quad (10)$$

where B_s is the maximum flux density at saturation. The Preisach model works only between $+1$ and -1 , so the flux density B_s is a scaling factor of the original values. Also the input value is normalized by $h(t) = H(t)/H_s$. Both, B_s and H_s are from real measurements.

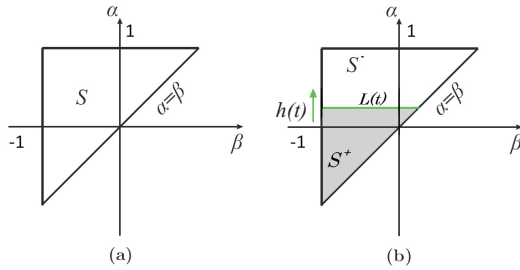


Figure 4: Preisach Plane

To reduce numerical effort, the Everett function is introduced

$$\mathcal{E}(h_{N-1}, h_N) = \text{sign}(h_{N-1}, h_N) \iint_{T_{h_{N-1}, h_N}} \wp(\alpha, \beta) d\alpha d\beta, \quad (11)$$

which leads to the final formulation

$$\mathcal{H}(h) = \mathcal{E}(-h_0, h_0) + \sum_{k=1}^N \mathcal{E}(h_{k-1}, h_k). \quad (12)$$

3.2. Graphical Representation

A illustrative graphical representation can be found in (Hegewald 2008) and will be used in this section. In Fig. 5 it is demonstrated how the operators $\gamma_{\alpha\beta}$ switch according to a specific input function $h(t)$. In the beginning all $\gamma_{\alpha\beta}$ are reset to 0. For a rising slope of $h(t)$, the $\gamma_{\alpha\beta}$ with the property $\alpha < h(t)$ are set to 1. For a falling slope of $h(t)$, the $\gamma_{\alpha\beta}$ with the $\beta > h(t)$ are reset to -1. This divides the Preisach plane S into one part with activated switching operators (S^+) and another part containing deactivated operators (S^-). The evaluation of the integral in (10) results in the hysteresis curve given in Fig. 5.c.

3.3. Weight Function and Identification Procedure

As already mentioned, the Preisach weight function defines the shape of the hysteresis curve and, therefore, has to be adapted to measured data. In principle, there are

two different methods. One possibility is to discretize the Preisach plane, which results in a finite number of weights $\wp(\alpha, \beta)$ that have to be identified. The other approach suggests an analytical function \wp_A with a small number of parameters to express the continuous weight function $\wp(\alpha, \beta)$. In the literature, e.g., (Consolo, Finocchiaro, Carpentieri, Cardelli, and Azzerboni 2006), a so called Lorentzian function with four parameters A, h, A_1 and A_2 can be mainly found.

3.3.1. Discretized Preisach Weights

Now, the identification problem is to determine the Preisach weights $\wp(\alpha, \beta)$. It has been shown in (Mayergoyz 2003), that this task can be solved by a family of symmetric minor loops. The first step is to discretize the Preisach plane into M supporting points. The supporting points are also responsible for the dimension of the weight matrix. The amount of discretization points in the Preisach plane is $n_{\wp} = \frac{1}{2}M(M+1)$. Figure 6 demonstrates the identification procedure.

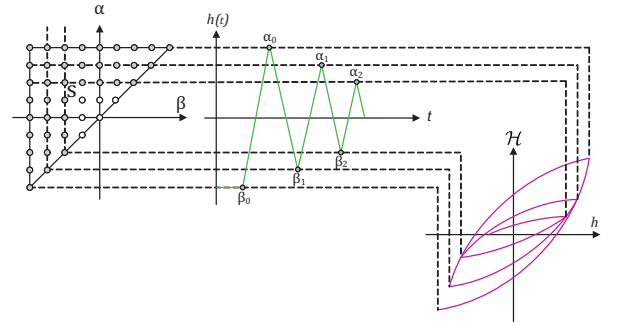


Figure 6: Parameter Identification Procedure \wp With ($M=9$) Supporting Points. The Gray Points in the Preisach Plane (On the Left Side) are Already Identified.

More discretization points means more of the symmetric minor loops to identify all of the reversal points α_1 to α_M and β_1 to β_M . Now, the discrete Preisach operator reads as

$$\mathcal{H} = \sum_{\lambda \in \Lambda} a_{\lambda} \mathcal{H}_{\lambda} \quad (13)$$

with \mathcal{H}_{λ} the simple relay operator having switching levels (α, β) . The amount of Λ consists of the index pairs (i, j) to characterize all switching thresholds α_i, β_j in the Preisach plane. By solving the least squares problem (Kaltenbacher and Kaltenbacher 2007)

$$\min \sum_{k=1}^{n_T} \left(\sum_{\lambda \in \Lambda} a_{\lambda} \mathcal{H}_{\lambda} [h_k] - B_k \right)^2 \quad (14)$$

with n_T the number of measurement points, we obtain the discrete Preisach weights. The advantage of this approach is that there exist distinct mathematical regulations for the identification of the weights, as described in (Mayergoyz 2003).

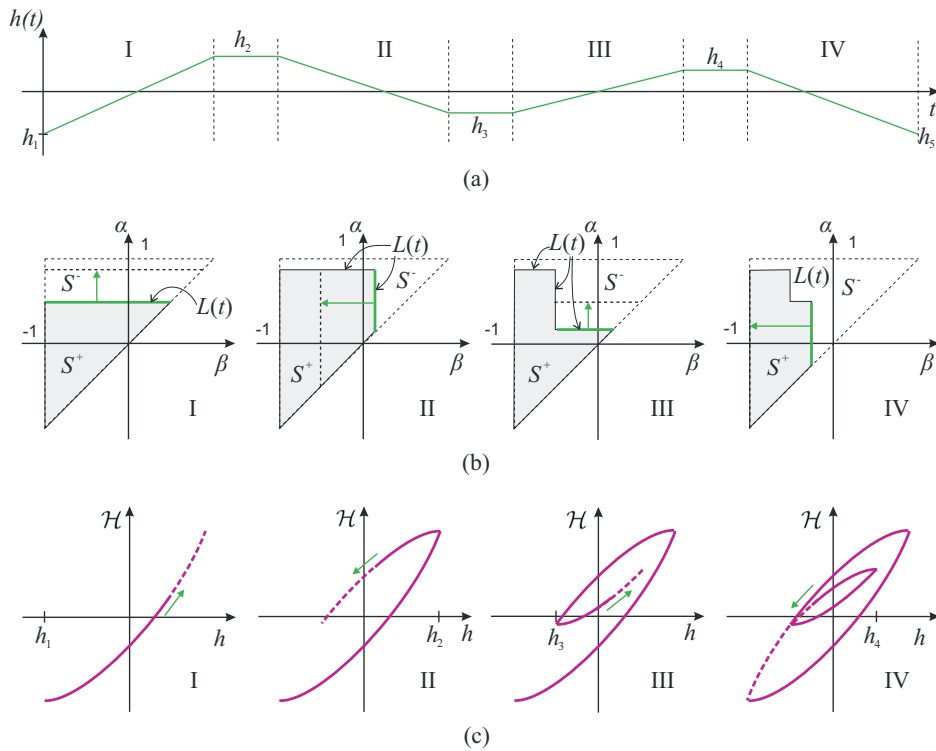


Figure 5: Graphical Representation of the Preisach Operator. (Hegewald 2008)

- (a): Example of the Time Behavior of an Input Signal $h(t)$,
- (b): Preisach Plane With Activated (S^+) and Not Activated (S^-) Switching Operators,
- (c): Resulting Hysteresis Curve.

3.3.2. Analytical Weight Function

As already mentioned before, a second method to express the weights $\wp(\alpha\beta)$ is an analytical function with a small number of parameters. We apply a Lorentzian weight function with four parameters $A, h, A1$ and $A2$. This analytical weight function can be further improved with help of an additional parameter η , which forms the corners of the hysteresis loop and makes the function suitable for a wide range of harder and softer magnetic materials (Sutor, Rupitsch, and Lerch 2010). Therewith, we arrive at the following analytical expression

$$\wp_{DAT}(\alpha, \beta) = \frac{A}{1 + (((\alpha + \beta)\sigma_1)^2 + ((\alpha - \beta - h(t_k))\sigma_2)^2)^\eta} \quad (15)$$

The parameters are obtained by applying the least-square curve fitting method using the optimization toolbox of Matlab.

4. EPSTEIN APPARATUS

The identification of the Preisach weights for the specific materials used in the transformer cores are based on measurements using an Epstein apparatus. The '25cm' Epstein apparatus consists of 4 coils with primary windings, secondary windings and the material sample as core. The sheets are stratified in stripes. The measurement setup represents in this way a transducer, whose characteristics are specified. The primary outer windings (N_1) are used to magnetize the material and the secondary inner windings (N_2) are needed for magnetic flux density de-

termination over the induced voltage U_2 . As the magnetic quantities are not measurable directly, the physical correct conversion into electric quantities must be guaranteed through the transducer principle. The steel sheet specimens are part of the transducer. For further details about this device and the measurement setup, please refer to the norm of the European Committee for Standardization (CEN) (CENELEC 2009).

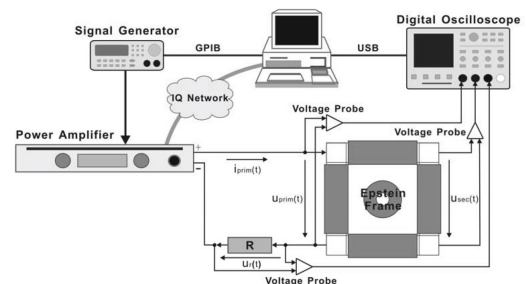


Figure 7: EpsteIn Setup for Measurements of Outer and Inner Hysteresis Loops.

5. FINITE NETWORK MODEL OF POWER TRANSFORMERS

Modeling magnetic components for use in circuit simulations can take several forms. The first approach, which is

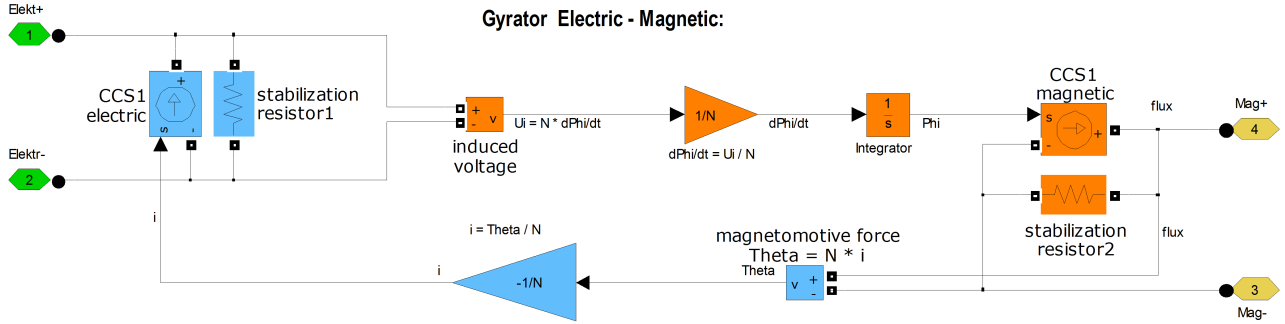


Figure 8: Gyration in Integral Form.

generally used, models each magnetic component as an ideal, linear component, using inductors with coupling coefficients to represent common flux paths. This can be extended to include nonlinear and even hysteretic couplings to model nonlinear and even hysteretic material behavior.

The technique, which we apply, is to decompose the system into two Kirchhoff circuits, one electric and one magnetic circuit (Brown, Ross, and Nichols 2001). Therewith, it is possible to simulate arbitrarily complex, nonlinear, hysteretic magnetic systems in the time domain and furthermore it can be used to consider the eddy currents. The hysteretic behavior of the inductance in the magnetic circuits is modeled by the classical Preisach operator as described in chapter 3.

5.1. Magneto-Electric Gyration

To couple the electric and magnetic circuit, we use a magneto-electric gyration as displayed in Fig. 9. This asymmetric component forms the basis of the interface between the magnetic and electric circuit, that allows to “push” devices from circuit to circuit. The dependent and

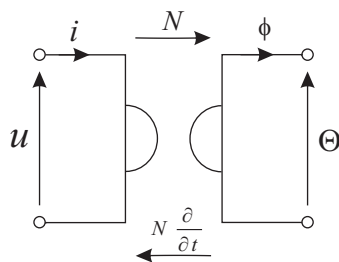


Figure 9: Gyration to Model the Connection Between the Electric and Magnetic Circuit.

independent variables in the electric network are voltage u and current i and the corresponding variables in the magnetic circuit are magnetomotive force Θ and flux ϕ . Therefore, the compound circuit is solved in terms for u , i , Θ and ϕ .

The components and equations (e.g. $u = Ri$, $u = L di/dt$) to model electric circuits are well known in comparison for modeling magnetic circuits. For this reason it is easier to transform components from the magnetic to

the electric domain or vice versa. For example, the magnetic inductor is the magnetic analog of a pure electric resistor. All the components generated by the transformations are given in Table 1. For further details about the gyration, we refer to literature, e.g. (Tellegen 1948; Brown, Ross, and Nichols 2001).

Table 1: Generalizing the Domain Equivalences (Brown, Ross, and Nichols 2001)

(a) From electric to magnetic				
Electric domain		to	Magnetic domain	
resistance	$u = iR$	to	inductance	$\Theta = \mathcal{L} \frac{d\Phi}{dt}; \mathcal{L} = \frac{N^2}{R}$
inductance	$u = L \frac{di}{dt}$	to	resistance	$\Theta = \mathcal{R} \Phi; \mathcal{R} = \frac{N^2}{L}$
capacitance	$i = C \frac{dU}{dt}$	to		$\Theta = N^2 C \frac{d^2\Phi}{dt^2}$

(b) From magnetic to electric				
Magnetic domain		to	Electric domain	
resistance	$\Theta = \mathcal{R} \Phi$	to	inductance	$u = L \frac{di}{dt}; L = \frac{N^2}{\mathcal{R}}$
inductance	$\Theta = \mathcal{L} \frac{d\Phi}{dt}$	to	resistance	$u = iR; R = \frac{N^2}{\mathcal{L}}$
capacitance	$\Phi = \mathcal{C} \frac{d^2\Theta}{dt^2}$	to	power source	$u = N^2 \mathcal{C} \frac{d^2i}{dt^2}$

The equations for the gyration in differential form are as follows

$$\begin{bmatrix} \Theta \\ u \end{bmatrix} = \begin{bmatrix} N & 0 \\ 0 & N \frac{\partial}{\partial t} \end{bmatrix} \begin{bmatrix} i \\ \phi \end{bmatrix}. \quad (16)$$

In some circuit simulators there may be problems with the differentiator and therefore one has to apply a modified formulation. One simple possibility is to use an inductivity as a substitute for the differentiator. A more sophisticated and stable method is to use the gyration with its integral form. This can be achieved by applying Faraday’s law in integral form

$$\phi = \frac{1}{N} \int u_i dt. \quad (17)$$

Therefore, the gyration equations rewrite as

$$\begin{bmatrix} \phi \\ i \end{bmatrix} = \begin{bmatrix} \frac{1}{N} \int \dots dt & 0 \\ 0 & \frac{1}{N} \end{bmatrix} \begin{bmatrix} u_i \\ \Theta \end{bmatrix}. \quad (18)$$

The used simulation model of the gyrator can be seen in Fig. 8. The orange highlighted blocks are the first row of (18) and the blue highlighted blocks are the second row. The connection ports for the electric circuit are green respectively yellow for the magnetic circuit. A stabilizing resistor has to be in parallel to the controlled current source to speed up the simulation.

5.2. Linear Circuit Model

First of all, we apply our developed model to a simple inductive circuit consisting of a resistor and a ideal inductor. Figure 10 shows the simple RL network when using our approach of the electric and magnetic circuit connected by a gyrator. The number of windings N to calculate the magnetic resistance ($\mathcal{R} = N^2/L$) is set to 1 (see also Tab. 1). Both forms of the gyrator (differential

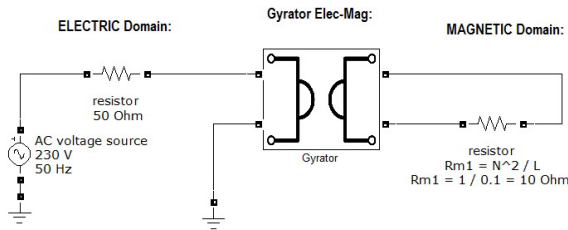


Figure 10: Simple Circuit with Gyrator.

as well as integral form) are used for the simulation to show the differences. As expected, the simulation results of the RL network with our approach and the standard one show exact the same behavior (see Fig. 11).

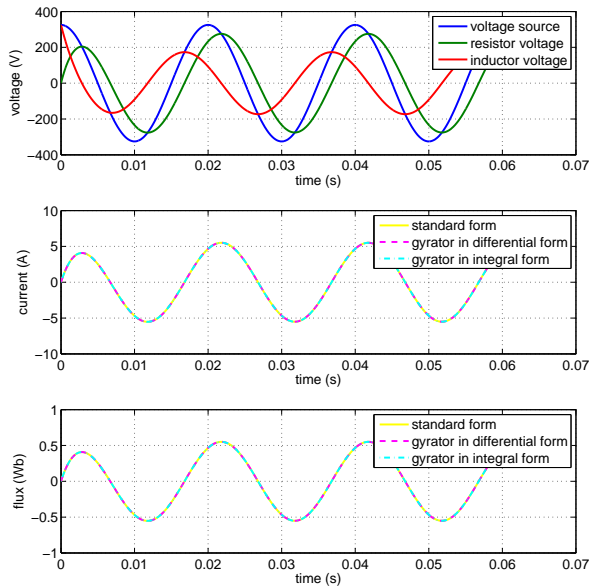


Figure 11: Simulation Results of the Simple RL Network With Gyrator.

5.3. Nonlinear Circuit Model

The linear circuit model can be seen as a linear transformer model with winding number $N = 1$. But, this model does not take the effects of saturation, hysteresis, and eddy currents into consideration. To model saturation, the linear reluctance has to be changed to a non-linear one. The subsystem of the non-linear resistor is shown in Fig. 12.

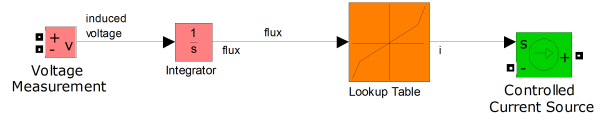


Figure 12: Model of a Nonlinear Inductance.

The current i flowing in the inductor is a nonlinear function of flux linkage ψ that, in turn, is a function of the induced voltage u_i appearing across its terminals, as described by Faraday's law. The voltage u_i is called self-induction and is given by the following relation

$$u_i = L \frac{di}{dt} = \frac{d\psi}{dt}, \quad (19)$$

or in integral form

$$\psi = \int u_i \cdot dt, \quad (20)$$

which results in

$$i = \frac{\psi}{L(\psi)}. \quad (21)$$

The model for the nonlinear inductance can therefore be implemented as a controlled current source, where current i is a nonlinear function of voltage u_i which will be computed with a look-up-table, as can be seen in Fig. 12. The red part in this figure describes (20), the look-up-table (orange) describes the flux-current characteristic and the controlled current source (green) converts the Simulink signal back to a SimPowerSystem signal.

5.4. Circuit Model with Hysteresis

The final step is to take the hysteresis behavior into account, which we do by the classical Preisach operator as it is described in chapter 3. Instead of the look-up-table, an interpreted MATLAB function block is used to describe the $i - \phi$ characteristics. The Preisach model works only between $+1$ and -1 and therefore the input and output values are scaled by their saturation values (i_{sat} & ϕ_{sat}). If the input signal raises beyond the saturation values, where the Preisach model can't work any longer, the simulation switch to the non-linear function

$$\phi(i) = c_1 \ln(c_2 i). \quad (22)$$

If the input signal falls below the saturation values, the simulation returns to the Preisach function. This detection of the input signal is included in the code inside the interpreted MATLAB function block. Another important block is the initial condition block (IC-block - red

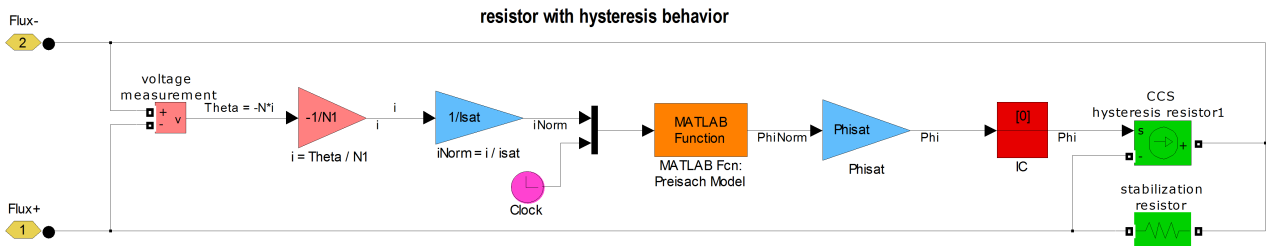


Figure 13: Resistor With Hysteresis Behavior.

block) to prevent algebraic loops in Simulink. This block provides an initial guess for the algebraic state variables in a loop.

Using a variable time stepping solver, another problem occur when using an interpreted MATLAB function block. The variable-step solvers dynamically increases or reduces the step size during the simulation by using its local error control to achieve the tolerances (Matlab 2001). Therefore all the parameters have to be stored with the correct time stamp which will be delivered by the clock (magenta).

Furthermore, the eddy currents are modeled by an additional magnetic inductance in series to the magnetic reluctance, where the inductance is calculated by $\mathcal{L} = N^2/R$ (see Tab. 1).

5.5. Three Phase Transformer

The single phase network can be easily extended now to a three phase network. There exist three different fluxes with different phase angles in this network. Therefore the three resistances with hysteresis behavior have their own Preisach function. Also included is the reluctance of the air path which is considered as constant. More details about modeling three phase transformers can be found in (Adly, Hanafy, and Abu-Shady 2003).

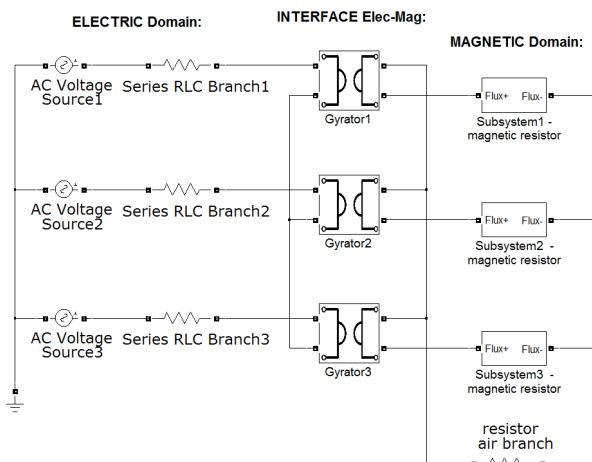


Figure 14: Three Phase Transformer.

6. RESULTS

For all circuit simulations the SimPowerSystems-Toolbox in MATLAB/Simulink® is used. The measured data for comparison with simulations are provided by a single phase transformer and a three phase transformer.

Two different simulations have been performed for comparison with the single phase transformer. The first one used the Preisach operator, where the identification procedure was based on 50Hz measurements, so that the eddy current losses are already included in the hysteresis curve. The second one used an identification procedure based on 10Hz measurements and an additional inductance in the magnetic circuit to model the eddy current losses. The results can be seen in Fig. 15. The simu-

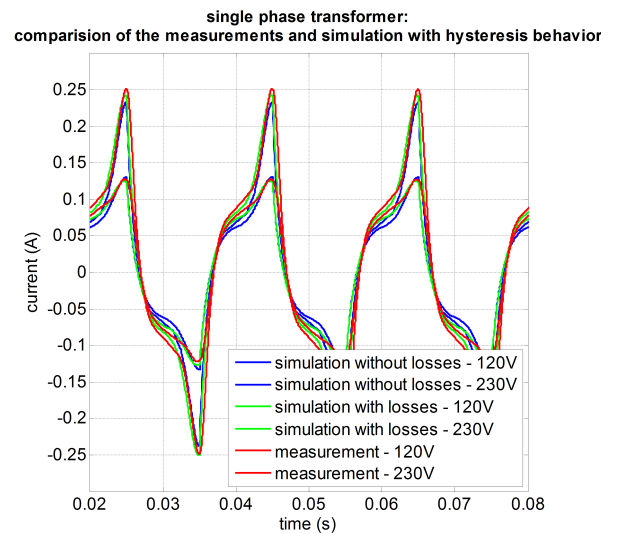


Figure 15: Results of the Single Phase Transformer.

lation results show acceptable agreement in comparison with measurements (red line). The simulation without additional inductance (blue line) show greater deviation in the real part as the simulation with inductance (green line).

The simulation model was extended to simulate three phase transformers as well. The results of the currents can be seen in Fig. 16. Here, the simulation results show quite good agreement in comparison with the measurements. Only the second phase has a larger deviation. It can be clearly seen that the three phases are influencing

each other and therefore the signal isn't sinusoidal any more. From the results it can be seen that our model may be used to design and optimize single- and three phase transformers used in electric power systems.

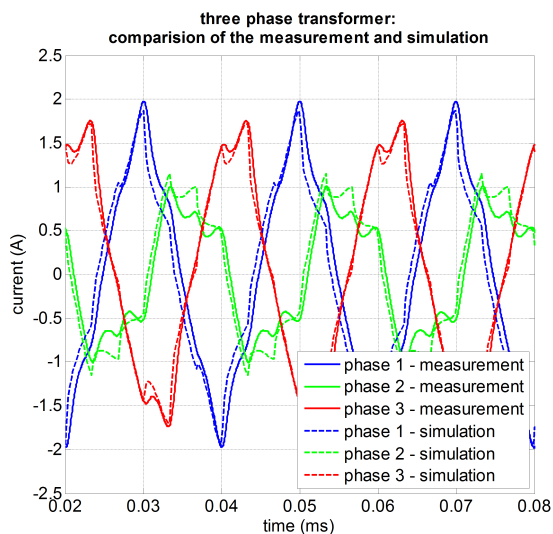


Figure 16: Results of the Three Phase Transformer.

6.1. Inrush Current

The inrush current waveforms are recorded by using an unloaded and demagnetized, single-phase transformer. Eddy currents are not taken into account. The switch-on angle for the transformer primary voltage is $\alpha = 0$.

A result for the inrush current is shown in Fig. 17, where the four first cycles of the simulated and the measured values are shown. By comparison of the measured and simulated values the agreement is very good.

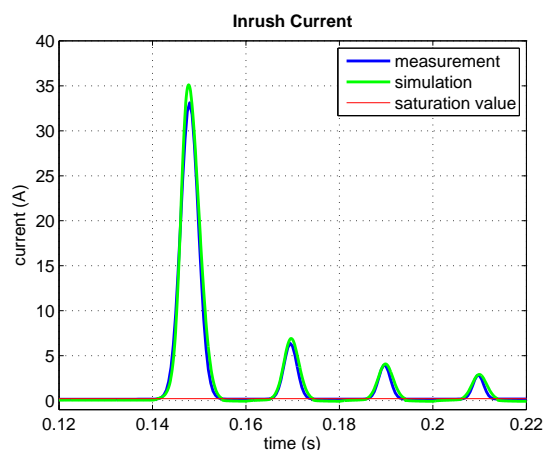


Figure 17: Results of the Inrush Current.

7. CONCLUSION

This paper demonstrated a simulation technique that allow mixed magnetic and electric systems to be analyzed in the time domain which is very useful for modeling single as well as three phase transformers. The Preisach

operator has been successfully incorporated into a transformer model with the help of a gyrator. For the validation of the model, simulation results of a single phase and a three phase transformer are compared to measurements. The simulations are in quite good agreement to the measurements.

REFERENCES

- Adly, A. A., Hanafy, H. H., and Abu-Shady, S. E., 2003. Utilizing preisach models of hysteresis in the computation of three-phase transformer inrush currents. *Electric Power Systems Research*, 65(3),233 – 238.
- Akçay, H. and Ece, D., 2003. Modeling of hysteresis and power losses in transformer laminations. *Power Delivery, IEEE Transactions on*, 18(2),487 – 492.
- Brown, A., Ross, J., and Nichols, K., 2001. Time-domain simulation of mixed nonlinear magnetic and electronic systems. *Magnetics, IEEE Transactions on*, 37(1),522 – 532.
- Casoria, S., Sybille, G., and Brunelle, P., 2003. Hysteresis modeling in the matlab/power system blockset. *Mathematics and Computers in Simulation*, 63(3-5), 237 – 248.
- CENELEC, 2009. Magnetische werkstoffe: Teil 2: Verfahren zur bestimmung der magnetischen eigenschaften von elektroblech und -band mit hilfe des epesteinrahmens.
- Chen, S.-D., Lin, R.-L., and Cheng, C.-K., 2005. Magnetizing inrush model of transformers based on structure parameters. *Power Delivery, IEEE Transactions on*, 20 (3),1947 – 1954.
- Consolo, G., Finocchio, G., Carpentieri, M., Cardelli, E., and Azzerboni, B., 2006. About identification of scalar preisach functions of soft magnetic materials. *Magnetics, IEEE Transactions on*, 42(4),923 – 926.
- Hagmann, G., 2001. *Grundlagen der Elektrotechnik*. AULA-Verlag.
- Hegewald, T., 2008. *Modellierung des nichtlinearen Verhaltens piezokeramischer Aktoren*. Thesis (PhD), Universitaet Erlangen-Nuernberg.
- Jungwirth, M., Baumgartinger, W., and Kaltenbacher, M., 2010. *Energie sparen durch Simulation in Energieeffiziente Mobilitaet*. Shaker Verlag.
- Kaltenbacher, B. and Kaltenbacher, M., 2007. Modelling and iterative identifictaion of hysteresis via Preisach operators in PDEs. In Kraus, J. and Langer, U. editors, *Lectures on Advanced Computational Methods in Mechanics*, chapter 1, pages 1–45. de Gruyter.
- Krasnoselskii, M. and Pokrovskii, A., 1989. *System with Hysteresis*. Springer Verlag.

- Matlab, M., 2001. *Simulink - Getting Started Guide*. The MathWorks GmbH, 3.0.1 edition.
- Mayergoyz, I., 2003. *Mathematical Models of Hysteresis and Their Applications Second Edition*. Academic Press.
- Sutor, A., Rupitsch, S., and Lerch, R., 2010. A preisach-based hysteresis model for magnetic and ferroelectric hysteresis. *Applied Physics A: Materials Science and Processing*, 100,425–430.
- Tellegen, B. D. H., 1948. The gyrator, a new electric network element. *Philips Research Reports*, 3(2),388–408.
- Theocharis, A., Miliadis-Argitis, J., and Zacharias, T., 2008. Single-phase transformer model including magnetic hysteresis and eddy currents. *Electrical Engineering (Archiv fur Elektrotechnik)*, 90,229–241.
- Visintin, A., 1994. *Differential Models of Hysteresis*, volume 111 of *Applied Mathematical Sciences*. Springer Verlag.

ACKNOWLEDGMENTS

This work was supported by European and Upper Austrian funds with grant number OOE 2007-13 (EFRE-REGIO 13).